

## Journal Pre-proofs

Epiphytic proliferation of *Zymoseptoria tritici* isolates on resistant wheat leaves

H.N. Fones, D. Soanes, S.J. Gurr

PII: S1087-1845(23)00053-1  
DOI: <https://doi.org/10.1016/j.fgb.2023.103822>  
Reference: YFGBI 103822

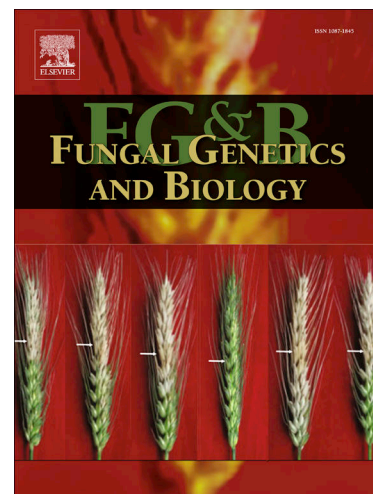
To appear in: *Fungal Genetics and Biology*

Received Date: 10 December 2022  
Revised Date: 4 June 2023  
Accepted Date: 15 June 2023

Please cite this article as: Fones, H.N., Soanes, D., Gurr, S.J., Epiphytic proliferation of *Zymoseptoria tritici* isolates on resistant wheat leaves, *Fungal Genetics and Biology* (2023), doi: <https://doi.org/10.1016/j.fgb.2023.103822>

This is a PDF file of an article that has undergone enhancements after acceptance, such as the addition of a cover page and metadata, and formatting for readability, but it is not yet the definitive version of record. This version will undergo additional copyediting, typesetting and review before it is published in its final form, but we are providing this version to give early visibility of the article. Please note that, during the production process, errors may be discovered which could affect the content, and all legal disclaimers that apply to the journal pertain.

© 2023 The Author(s). Published by Elsevier Inc.



# 1 **Epiphytic proliferation of *Zymoseptoria tritici* isolates on resistant wheat leaves.**

2 **Fones, H.N.<sup>1\*</sup>, Soanes, D.<sup>2</sup> and Gurr, S.J.<sup>1,3\*</sup>**

3 **1** - Biosciences, University of Exeter, Exeter, UK

4 **2** - University of Exeter Medical School, Exeter, UK

5 **3** - Department of Biosciences, Utrecht University, Utrecht, the Netherlands

6 \*For correspondence: [h.n.eyles@exeter.ac.uk](mailto:h.n.eyles@exeter.ac.uk) or [s.j.gurr@exeter.ac.uk](mailto:s.j.gurr@exeter.ac.uk)

## 7 **Abstract**

8 The wheat pathogen *Zymoseptoria tritici* is capable of a long period of pre-invasive epiphytic growth.  
9 Studies have shown that virulent isolates vary in the extent, duration and growth form of this  
10 epiphytic growth, and the fungus has been observed to undergo behaviours such as asexual  
11 reproduction by budding and vegetative fusion of hyphae on the leaf surface. This epiphytic  
12 colonisation has been investigated very little during interactions in which an isolate of *Z. tritici* is  
13 unable to colonise the apoplast, as occurs during avirulence. However, avirulent isolates have been  
14 seen to undergo sexual crosses in the absence of leaf penetration, and it is widely accepted that the  
15 main point of distinction between virulent and avirulent isolates occurs at the point of attempted  
16 leaf penetration or attempted apoplastic growth, which fails in the avirulent case. In this work, we  
17 describe extensive epiphytic growth in three isolates which are unable or have very limited ability to  
18 invade the leaf, and show that growth form is as variable as for fully virulent isolates. We  
19 demonstrate that during certain interactions, *Z. tritici* isolates rarely invade the leaf and form  
20 pycnidia, but induce necrosis and are able to achieve higher epiphytic biomass than virulent isolates  
21 during asymptomatic growth, and may undergo very extensive asexual reproduction on the leaf  
22 surface. These findings have implications for open questions such as whether and how *Z. tritici*  
23 obtains nutrients on the leaf surface and the nature of its interaction with wheat defences.

24 **Key words:** *Zymoseptoria tritici*, epiphyte, surface proliferation, virulence, blastosporulation

## 25 **Highlights**

- 26 • *Zymoseptoria tritici* isolates inoculated onto wheat on which they are not fully virulent are  
27 generally unable to enter the leaves, but instead proliferate epiphytically.
- 28 • These isolates induce early defence responses, leading to leaf necrosis, albeit to a lesser  
29 extent than seen in fully virulent isolates. They produce pycnidia very rarely, but not never.  
30 We named this isolate-cultivar interaction 'Necrosis-inducing with rare pycnidiation' (NIRP).
- 31 • Epiphytic growth by NIRP isolates can produce more biomass than early invasive growth  
32 during 'stealth biotrophy'. This advantage is later lost, because the NIRP isolates produce so  
33 few pycnidia in comparison to fully virulent isolates.
- 34 • We speculate that epiphytic proliferation in NIRP interactions may help to maintain the NIRP  
35 isolates' genes in field populations of *Z. tritici*.

36  
37 **Funding:** This work was funded by a BBSRC grant awarded to SJG and a UKRI Future Leaders  
38 Fellowship (MR/T021608/1) awarded to HNF.

39

40

41 **Introduction**

42 *Zymoseptoria tritici* is an ascomycete fungus that causes the wheat disease Septoria Tritici Blotch  
43 (STB). STB is the most important pathogen of temperate-grown wheat, causing yield losses of up to  
44 £200M per year in the UK alone and necessitating the extensive – and expensive – use of fungicides  
45 to protect even resistant wheat cultivars (Fones & Gurr, 2015). Resistance to STB is often  
46 quantitative, although a number of resistance genes, termed *stb* genes, are also known (Saintenac *et al.*,  
47 2018; Mekonnen *et al.*, 2021). It has been reported that the defining feature of interactions  
48 between avirulent isolates and resistant wheat cultivars is that fungal growth is arrested at the point  
49 of stomatal penetration (Kema *et al.*, 1996; Battache *et al.*, 2022) due to the accumulation of  
50 hydrogen peroxide (Shetty *et al.*, 2003), cell wall strengthening, metabolic changes and production  
51 of apoplastic defences such as *PR*-proteins (Rudd *et al.*, 2015; Yang *et al.*, 2015), or promotion of  
52 stomatal closure (Battache *et al.*, 2022).

53 Prior to penetration, however, the fungus may colonise the leaf surface. Epiphytic colonisation of  
54 the leaf has been previously documented in interactions between virulent isolates and susceptible  
55 wheat (Fones *et al.*, 2017; Haueisen *et al.*, 2019; Fantozzi *et al.*, 2021). Our previous work showed  
56 that the reference isolate, *Z. tritici* IPO323, germinates asynchronously to form hyphae which grow  
57 randomly across the leaf surface, penetrating stomata as they are encountered. Rare stomatal  
58 penetration events were observed as soon as 1 dpi, but significant ingress into the leaf was not  
59 observed until around ten days after inoculation, once sufficiently large hyphal networks had  
60 developed for growing tips to encounter stomata frequently (Fones *et al.*, 2017). Fantozzi *et al.*  
61 (2021) quantified this asynchronicity in the development of *Z. tritici* IPO323 on and in the leaves of  
62 susceptible wheat. Their work showed that multiple stages of infection co-exist within a leaf sample,  
63 with some fungi remaining in the ‘surface resting’ and ‘surface exploration’ stages of infection  
64 throughout an 18-day time course. Haueisen *et al.* (2019) also described surface colonisation by  
65 virulent isolates, finding variation in the extent of this epiphytic growth among isolates that are not  
66 significantly different in virulence. Isolates differed in the speed of symptom development, but more  
67 extensive epiphytic growth did not indicate delayed disease (Haueisen *et al.*, 2019).

68 This epiphytic growth has so far not been investigated in detail in interactions where the *Z. tritici*  
69 isolate is unable or has limited ability to penetrate stomata and colonise the host apoplast. The  
70 prevention of stomatal penetration is of fundamental importance in wheat defences against *Z. tritici*.  
71 This, however, does not preclude the possibility that fungal germination and epiphytic growth prior  
72 to penetration might occur on resistant wheat cultivars. The only study, to our knowledge, which has  
73 explicitly compared pre-penetration growth in isolates of contrasting virulence was that of Siah *et al.*  
74 (2010). These authors noted that pre-penetration growth in a weakly pathogenic isolate was similar  
75 to that of a fully pathogenic isolate (Siah *et al.*, 2010). Further, both blastosporulation (microcycle  
76 conidiation) and anastomosis (vegetative hyphal fusion) have been observed on the leaf surface  
77 within 48 h of inoculation with virulent pycnidiospores (Francisco *et al.*, 2019). It has also been  
78 reported that both virulent/avirulent (Kema *et al.*, 2018) and avirulent/avirulent (Orellana-Torrejon  
79 *et al.*, 2022) isolate pairs can cross on the wheat leaf, even without causing symptoms. Taken  
80 together, these findings suggest that epiphytic growth and reproduction – asexual and sexual – can  
81 occur in *Z. tritici* even when the host wheat cultivar is resistant to infection.

82 In this work, we test the hypotheses that virulent and avirulent isolates are equally able to grow as  
83 epiphytes, and that weakly virulent or avirulent isolates would display similar variability in the extent  
84 of epiphytic growth as seen in virulent isolates (Haueisen *et al.*, 2019). Using confocal microscopy of  
85 GFP-tagged *Z. tritici*, complemented by SEM and qPCR-based *Z. tritici* quantitation, we assess the  
86 epiphytic growth of six isolates which we show to have different degrees of virulence on the wheat

87 cultivar Galaxie. We also test the hypothesis that variation in the extent of epiphytic colonisation is  
88 independent of plant defence responses by quantifying the production of the ROS, superoxide,  
89 known to have a direct defensive role as well as being central to defence signalling in plants.

## 90 **Materials and Methods**

### 91 ***Zymoseptoria tritici* isolates**

92 The *Z. tritici* isolates used in this study were kindly provided by Prof. Gert Kema and Prof Gero  
93 Steinberg. Strains IPO323 and IPO94269 were isolated in the Netherlands and have been widely used  
94 in studies of *Z. tritici*, with IPO323 commonly regarded as the reference isolates for work on this  
95 fungus (Kema *et al.*, 2002; Goodwin *et al.*, 2007; 2011). IPO97001 was isolated in the Czech  
96 Republic (Kema, G, pers. comm). Strains T5, T23 and T39 were all isolated in the USA, T5 from  
97 Minnesota and the others from North Dakota (Kema, G, pers. comm). All strains were isolated from  
98 bread wheat. Strains of each isolate expressing cytosolic GFP were provided by Dr Sreedhar Kilaru. In  
99 each case, the GFP construct was integrated into the *sid1* locus according to the methodology  
100 published in Kilaru *et al.* (2015).

### 101 **Wheat plants and inoculation of wheat with *Z. tritici*.**

102 The wheat variety used in this work was Galaxie (Fenaco, Bern, Switzerland). This cultivar is known  
103 to be susceptible to isolate IPO323 (e.g. Fones *et al.*, 2017; Fantozzi *et al.*, 2021). Wheat seeds were  
104 sown on damp John Innes No. 2 compost in a 24-cell seed tray and thinned to 2 plants per cell  
105 following germination. Seedlings were kept under cloches in a growth chamber at 20 °C, 80% RH,  
106 12 h light until germination (4 days), when cloches were removed.

107 Inoculations were carried out on 14 day-old plants. Spore suspensions were filtered through two  
108 layers of sterile Miracloth to remove hyphal or large branching structures. Fully expanded leaves  
109 were marked at the base and a  $10^7$  cfu/ml suspension of filtered *Z. tritici* spores in 0.1% (v/v) Tween-  
110 20 applied with a paintbrush. Inoculated plants were returned to the growth chamber and covered  
111 with cloches for the first 72 h. Cloches were then removed, and plants maintained until 28 days post  
112 inoculation (dpi).

### 113 **Assessment of symptoms.**

114 Symptom development was assessed by harvesting three inoculated leaves per isolate at 7, 14, and  
115 21 dpi. Harvested leaves were rehydrated for 30 mins in tap water if necrotic, dried and taped onto  
116 white paper for high-resolution (800 dpi) scanning. Three uninfected control leaves were also  
117 scanned. Scanned images were analysed leaf by leaf using colour thresholding in ImageJ (Abramoff  
118 *et al.*, 2004). First the white background was removed and the leaf area measured, and then  
119 progressive thresholding steps in HSB colour space were used to exclude healthy (greens) and  
120 chlorotic (yellows) areas, allowing areas of necrotic, chlorotic and healthy tissue to be calculated.  
121 These were then expressed as percentages of the total leaf area. Three independent replicate  
122 experiments were carried out.

### 123 **Assessment of pycnidiation**

124 Pycnidiation was assessed by harvesting 4-12 inoculated leaves per isolate at 28 dpi. Harvested  
125 leaves were rehydrated for 30 mins in tap water if necrotic, dried and taped onto white paper for  
126 high-resolution scanning. Scanned images were analysed leaf by leaf using colour thresholding in  
127 ImageJ (Abramoff *et al.*, 2004). First the white background was removed, and the leaf area  
128 measured. Following this, thresholding in HSB colour space was used to selected black areas of the  
129 image. These were then further restricted to a selection of near circular areas of the appropriate size

130 for pycnidia, and enumerated, using the 'analyse particles' function in ImageJ. Data were then  
131 expressed as pycnidia/cm<sup>2</sup> leaf. Three independent replicate experiments were carried out.

### 132 **Confocal Laser Scanning Microscopy (CLSM)**

133 Samples of leaves inoculated with GFP-tagged strains of all fungal isolates were mounted in 0.1%  
134 (v/v) phosphate buffered saline (PBS, pH 7) and if necrotic, stained with 5 µl 0.05% (w/v) propidium  
135 iodide (PI). Confocal microscopy was carried out using argon laser emission at 500 nm with detection  
136 in 600–630 nm (chlorophyll/PI, red) and 510–530 nm (GFP, green), using a Leica SP8 confocal  
137 microscope.

### 138 **Scanning Electron Microscopy (SEM)**

139 Small samples of inoculated leaves were rapidly frozen in liquid nitrogen slush. Samples were then  
140 etched and sputter-coated for visualisation. This procedure was carried out using a Jeol JSM-6390LV  
141 cryo-SEM rig with Gatan Cryo-transfer system.

### 142 **qPCR**

143 For quantification of *Z. tritici* in and on inoculated leaves by qPCR, inoculations were carried out as  
144 for other infection experiments, with at least two leaves on each of 30 plants infected with each  
145 isolate. Each leaf sample consisted of at least five leaves from separate plants. DNA extracted from  
146 infected leaf material was used as a template for qPCR of a *Z. tritici* specific gene, using the primer  
147 pair ST-rRNA F/R, developed by Guo *et al.* (2006), with the PCR cycling conditions contained in that  
148 work. Leaf material was either used as sampled, to measure the total fungal DNA associated with the  
149 leaf sample, or was vigorously shaken in 0.1% (w/v) Tween-20 for 1 min. This has previously been  
150 demonstrated to remove >90% of fungus from the leaf surface (Fones *et al.*, 2017) and thus, these  
151 'washed' samples allowed the detection of DNA almost exclusively from fungus internal to the leaf.  
152 qRT-PCR was carried out on three replicate samples for each isolate in both the 'washed' and  
153 'unwashed' condition, plus three replicate uninfected control leaf samples, each consisting of five  
154 leaves pooled from separate plants. Two independent replicate experiments were carried out.  
155 Primer sequences are given in Table S1.

### 156 **Assessment of Reactive Oxygen Species production by inoculated wheat**

157 For the measurement of superoxide, harvested leaves were submerged in 0.1% (w/v) nitroblue  
158 tetrazolium (NBT) (Love *et al.*, 2005) overnight, before clearing by boiling in methanol. Cleared,  
159 stained leaves were scanned at high resolution and images were analysed in HSB colour space in  
160 ImageJ to measure the percentage of the total leaf area that had been stained blue by NBT. For each  
161 isolate and time point, a minimum of three leaves (3-6) were scanned and analysed, and the  
162 experiment was repeated three times independently.

### 163 **Statistical analysis**

164 Unless otherwise stated in the relevant figure legend, data presented represent means of three or  
165 more independent experiments, and error bars show standard error of the mean (SE). Where  
166 multiple pairwise comparisons were required, Bonferroni corrected *t*-tests were used. Otherwise,  
167 Analysis of Variance tests were used with Tukey's simultaneous comparisons. Results of *t* tests are  
168 shown as asterisks (\*, *p*<0.05; \*\*, *p*<0.01; \*\*\*, *p*<0.001 or NS, *p*≥0.05) in figures. Results of Tukey's  
169 tests are shown as letters above data points in figures, where different letters represent significantly  
170 differing datapoints. Further details of statistical tests, such as complete ANOVA tables, are given in  
171 Supplemental Info S1.



172 **Sequencing and genomic analyses**

173 Library preparation, sequencing and de novo assembly was performed by Exeter Sequencing Service.  
174 Genomic DNA was extracted 5-day old *Z. tritici* grown on YPD agar using a standard phenol-  
175 chloroform extraction procedure. DNA was and quantified by Qubit assay (Thermo Fisher Scientific).  
176 DNA was fragmented to ~500 bp sections and Illumina sequencing libraries prepared using Nextflex  
177 Rapid DNaseq kit for Illumina sequencing (BioScientific) with adapters containing indexes and 5–8  
178 cycles polymerase chain reaction (PCR) (Head *et al.*, 2014). Library quality was determined using  
179 D1000 screen-tapes (Agilent) sequenced using a combination of Illumina MiSeq and/or Illumina  
180 HiSeq 2500. Trimmed reads were aligned against *Z. tritici* reference genome IPO323 (Goodwin *et al.*,  
181 2011) using BWA (Li & Durbin 2009). Pileup files was created using SAMtools mpileup (Li, 2011). A  
182 custom perl script was used to call shared SNPs from essential chromosomes 1-13 at 95% minimum  
183 base identity and minimum 10 x coverage for each position across all the strains. This produced  
184 627,536 SNPs. Bases at SNP sites were used to produce a pseudosequence for each strain that was  
185 used to infer phylogenetic relationship with PhyML (Guindon *et al.*, 2010) (100 bootstraps, GTR  
186 nucleotide substitution model, 8 substitution rate categories, gamma shape parameter and  
187 proportion of invariant sites estimated).

188

189 **Results:**

190

191 **European *Z. tritici* isolates tested are fully virulent on the susceptible European bread wheat,**  
192 **Galaxie, but American isolates induce necrosis without producing pycnidia..**

193 In order to determine the virulence of the isolates IPO323, IPO94269, IPO97001, T5, T23 and T39 on  
194 Galaxie, infections were carried out and both symptom development and pycnidiation measured  
195 (Fig. 1). Symptom development was the same in all isolates up to 7 days post inoculation (dpi) (Fig  
196 1A; ANOVA,  $p = 0.7022$ ) and there were no significant differences at 14 dpi (Fig 1B, ANOVA,  $p =$   
197  $0.6418$ ). However, when the percentage leaf area showing necrosis was compared between isolates  
198 at 21 dpi, highly significant differences were detected (ANOVA,  $p < 0.0001$ ). These differences  
199 appear to be due to the much more extensive necrosis seen in the European strains (Fig 1C). Tukey's  
200 simultaneous pairwise comparisons confirm that all of the European isolates show significantly more  
201 necrosis than all of the American isolates (for detailed statistical results, see Supplementary Info S1).  
202 Control (uninoculated) leaves did not show necrosis, indicating that all fungal isolates induce  
203 necrosis. However, for American isolates this necrosis is not associated with pycnidiation, and may  
204 instead reflect plant defence. American isolates T5, T23 and T39 were, in fact, almost completely  
205 unable to sporulate in Galaxie, producing on average 12.8 pycnidia/cm<sup>2</sup> leaf, as opposed to an  
206 average of 145.7 pycnidia/cm<sup>2</sup> leaf on average for European isolates IPO323, IPO94269 and  
207 IPO97001. There were differences in pycnidiation among the isolates (ANOVA,  $p < 0.0001$ ; Fig 1D).  
208 European isolates differed from each other and from the uninoculated control, , whereas none of the  
209 American isolates differed significantly from the uninoculated control (Tukey's simultaneous  
210 comparisons; for detailed statistical results, see Supplementary Info S1). For simplicity, we adopt  
211 the shorthand 'fully virulent' ('FV') and 'Necrosis-inducing with rare pycnidiation' ('NIRP') to  
212 describe European vs American isolates in the rest of this report, although of course it must be  
213 noted that these appellations apply only to their interactions with Galaxie. The American isolates are  
214 likely to be more able to complete their lifecycle and produce pycnidia on certain other wheat  
215 cultivars, while it is understood that the European isolates are avirulent on some wheat cultivars. For  
216 instance, IPO323 is avirulent on cultivars carrying *stb6*. Therefore, we emphasise that the FV and  
217 NIRP phenotypes described here are specific to these particular isolate-cultivar interactions.

218 Differences between the two groups of isolates are likely to be attributable to the geographical  
219 separation of these groups. We sequenced the genomes of the six isolates and identified SNPs on  
220 the 13 core chromosomes (see Supplemental Info S2). Pairwise comparisons showed a minimum of  
221 142,000 SNPs (T5/T39), while the maximum was 257,000 (IPO97001/T39). A pseudosequence tree  
222 derived from these SNPs (Fig. S1) shows that, as expected, European (fully virulent) isolates cluster  
223 together, as do American (NIRP) isolates.

224 **'NIRP' *Z. tritici* isolates that rarely penetrate into the internal spaces of the leaf nevertheless show**  
225 **extensive proliferation on the wheat leaf surface.** To reveal the underlying reasons for the  
226 symptoms shown and the scarcity of pycnidiation in the American isolates, GFP-expressing strains of  
227 all isolates were inoculated onto Galaxie leaves and viewed using confocal laser scanning microscopy  
228 (CLSM) at multiple time points throughout infection. In parallel, wildtype isolates were observed by  
229 scanning electron microscopy (SEM). Representative CSLM and SEM images of each isolate at 7 and  
230 14 dpi are shown in Fig. 2. Differences in the extent of leaf surface colonisation are apparent  
231 between the isolates, as are differences in the number of cells in yeast-like vs hyphal growth forms.  
232 In particular, isolate T23 shows extensive hyphal growth on the leaf surface, while T39 shows a  
233 proliferation of yeast like cells, from clumps at 7 dpi to extensive leaf surface coverage by 14 dpi. By  
234 contrast, the fully virulent isolates show internal colonisation by 14 dpi, with comparatively little  
235 increase in surface coverage between 7 and 24 dpi. This is illustrated in more detail in Fig. 3, where  
236 images are shown for the reference isolate IPO323 (FV) in comparison to T39 (NIRP) throughout the  
237 time course of infection. Initial inoculum at 0 dpi looks similar in these isolates and there are no  
238 visually apparent differences at 3 dpi. By 7 dpi, however, the majority of IPO323 cells are in the  
239 hyphal form, while yeast-like cell proliferation is observed in T39. From day 10 onwards, IPO323 can  
240 be visualised inside the leaf as well as on the leaf surface, but T39 cannot. Yeast-like surface  
241 proliferation continues in T39 at the later time points, while IPO323 colonises the internal spaces of  
242 the leaf and, by day 18, begins to form pycnidia.

243 In order to quantify these differences in leaf colonisation and fungal growth, multiple CSLM images  
244 were obtained of each isolate on or in the leaf at multiple time points after inoculation. These  
245 images were analysed to determine how many individual fungi contained one or more cells in the  
246 hyphal state (Fig. 4A) or remained wholly on the leaf surface, with no stomatal ingress or  
247 colonisation of internal leaf spaces (Fig 4B). Germination of cells to form hyphae occurred at  
248 different rates for different isolates, with differences apparent by day 3 (ANOVA,  $p = 0.04525$ ).  
249 However, all isolates showed the ability to form hyphae. The two groups of isolates (FV vs NIRP)  
250 could not be distinguished based on the rate of hyphal formation on at any of the time points  
251 analysed ( $t$ -tests comparing means for isolate groups: 3 dpi,  $p = 0.269$ ; 7 dpi,  $p = 0.963$ ; 10 dpi,  $p =$   
252  $0.626$ ). Unlike hyphal formation, however, leaf penetration separated the two groups of isolates ( $t$ -  
253 tests comparing means for isolate groups: 10 dpi,  $p = 0.0339$ ; 12 dpi,  $p = 0.0496$ ). In fact, no internal  
254 hyphae were observed for any NIRP isolate throughout the time course (Fig 4B).

255 In addition to microscopic analyses, DNA extracted from infected leaf material was used as a  
256 template for qPCR of a *Z. tritici* specific gene, comparing washed and unwashed leaf material.  
257 Washing removes >90% of surface fungus (Fones *et al.*, 2017), allowing surface vs internal fungal  
258 colonisation to be distinguished in this way. At 7dpi, qPCR results show low quantities of *Z. tritici*  
259 DNA in all samples, regardless of isolate and washing (Fig. 5A). Despite this, washing the leaves led  
260 to a significant reduction in *Z. tritici* DNA detection (ANOVA, washed vs unwashed, 7 dpi:  $p < 0.0001$ ).  
261 At 14 dpi, *Z. tritici* DNA was detected for all isolates in unwashed leaves, with NIRP isolates showing  
262 up to 4 x as much as fully virulent isolates (Fig. 5B;  $p < 0.0001$ ). For the fully virulent isolates, washing  
263 did not significantly alter the amount of *Z. tritici* DNA detected at 14 dpi (Fig. 5B; ANOVA  $p = 0.995$ ).  
264 However, for NIRP isolates, washing caused an up to 59-fold reduction in *Z. tritici* DNA detection (Fig  
265 5B; ANOVA  $p < 0.0001$ ). These results are consistent with the microscopic analysis, indicating that  
266 the NIRP isolates are able to proliferate on the leaf surface but rarely enter the internal spaces of the

267 leaf, while fully virulent isolates enter the leaf by 14 dpi and undergo less leaf surface proliferation.  
268 Comparing the amount of *Z. tritici* DNA detected in washed leaves at 14 dpi shows that internal  
269 proliferation occurred in the fully virulent isolates but not in the NIRP isolates (Fig 5B; ANOVA  
270 0.00235). Again, this is consistent with the microscopic analysis. Taken together, these results  
271 indicate that while the three fully virulent isolates invaded Galaxie in the manner normally  
272 considered characteristic for virulent *Z. tritici* on susceptible wheat, the three NIRP isolates were  
273 minimally invasive and rarely able to complete their lifecycle to pycnidiation in Galaxie. Instead, they  
274 undergo surface proliferation.

#### 275 **NIRP isolates elicit different wheat defence responses to FV isolates.**

276 To investigate the response of Galaxie wheat to the NIRP isolates of *Z. tritici*, we investigated ROS  
277 signalling. Staining inoculated leaves with nitroblue tetrazolium (NBT) revealed that at 1 dpi, NIRP  
278 isolates already elicit slightly higher ROS production than the FV isolates (ANOVA,  $p = 0.00282$ ). This  
279 difference no longer apparent by 2 dpi ( $t$ -test,  $p = 0.2257$ ) and is reversed, but remains non-  
280 significant, at 7 dpi ( $t$ -test,  $p = 0.183$ ). This reversal, with the reduction of ROS response elicited by  
281 avirulent isolates to less than that seen in response to the fully virulent isolates, is significant at 14  
282 dpi ( $t$ -test,  $p = 0.00085$ ). This pattern of response at 14 dpi was also seen in expression of the  $\beta$ -1,3-  
283 glucanase gene, whose expression is associated with fungal leaf penetration and the resulting wheat  
284 defence response (Figure S2; see Supplementary Info S2 for methods).

285

#### 286 **Discussion**

287 In this work, we have shown that there are interactions between certain wheat cultivars and isolates  
288 of the fungal wheat pathogen *Zymoseptoria tritici* in which the *Z. tritici* isolate is able to survive and  
289 reproduce on the leaf surface when despite being unable to colonise the apoplastic spaces inside the  
290 leaf. Given that the NIRP phenotype is seen in American isolates which are more closely related to  
291 each other than to isolates from Europe, it is possible that the NIRP phenotype reflects poor  
292 adaptation of American isolates to the European wheat Galaxie. However, such poor adaptation to  
293 available hosts might also be expected in the field when, for example, a new elite cultivar is  
294 introduced. It will be important to determine whether the NIRP phenotype is also seen in any field  
295 isolates on the wheat varieties from which they were isolated.

#### 296 **Epiphytic proliferation is common to fully virulent and NIRP interactions.**

297 Confocal and scanning electron microscopy were used to visualise three fully virulent and three NIRP  
298 isolates on and in the leaves of Galaxie wheat (Figs1-2). As can be seen in Fig. 2, epiphytic fungal  
299 proliferation was clearly visible in every isolate at both 7 and 14 dpi. This is similar to the findings of  
300 Siah *et al.*, 2010, who showed that both a fully- and a weakly virulent isolate grew similarly on the  
301 leaf surface prior to penetration. However, by comparing multiple *Z. tritici* isolates, we show that  
302 the form and extent of epiphytic growth in NIRP isolates are as variable as for fully virulent isolates.  
303 In particular, the isolate T39 showed extensive blastosporulation (microcycle conidiation/budding)  
304 on the leaf surface, which persisted throughout the infection period (Fig. 3). In contrast, the  
305 reference isolate IPO323 was less visible on the leaf surface from 10 dpi onwards, by which time it  
306 had penetrated, and begun to colonise, the apoplast. Quantitative analysis showed that the fully  
307 virulent isolates could not be distinguished from the NIRP isolates by growth form. Indeed, the  
308 percentage of cells in hyphal vs yeast like forms at each timepoint differed as much within as  
309 between isolate groups (Fig. 4A). Differences in the proportion of hyphal vs yeast-like individuals  
310 may arise from differences in the rate at which initial blastospore inoculum germinates to produce  
311 cells in the hyphal growth form, but also in the rate at which blastosporulation occurs on the leaf



312 surface to form new yeast-like cells. Both IPO323 and T23 rapidly germinate and reach around 90%  
 313 hyphal growth form by 10 dpi (Fig 4A), in line with previously published data for IPO323 (Fones *et al.*,  
 314 2017; Fantozzi *et al.*, 2021). Other isolates show a maximum of 30-60% hyphal cells (Fig 4A) in the  
 315 same time period, reflecting either reduced germination (T5, IPO97001) or increased  
 316 blastosporulation (IPO94269, T5, T39), as can be seen in figures 2 and 3.

317 **Ability to penetrate stomata and colonise the apoplast is essential for pycnidiation, but not for**  
 318 **increases in fungal biomass.**

319 Unlike germination, leaf penetration provides a clear separation between the fully virulent and NIRP  
 320 isolates. No NIRP strain was able to colonise the apoplast, with all observed fungal cells being wholly  
 321 on the leaf surface at all time points analysed (Figure 4B). This is in line with previous findings that  
 322 abortive penetration events, ending with the death or the cessation of growth in the hypha  
 323 attempting penetration, are characteristic of incompatible *Zymoseptoria*-wheat interactions (Shetty  
 324 *et al.*, 2003; Yang *et al.*, 2015; Battache *et al.*, 2022), of the interaction between wheat and other  
 325 *Zymoseptoria* species which are not pathogenic on this plant (Poppe *et al.*, 2015), and of the  
 326 interaction of *Z. tritici* with non-wheat grasses (O'Driscoll *et al.*, 2015; Habig *et al.*, 2017). This is  
 327 believed to be the result of plant defences activated following the detection of the fungus in the  
 328 apoplast (Battache *et al.*, 2022). In line with this, we found no significant increase in NBT staining for  
 329 superoxide in fully virulent isolates compared to NIRP isolates at times up to and including 7 dpi. At  
 330 1 dpi, there was in fact a significantly high response to the NIRP isolates, but this was short-lived (no  
 331 difference seen at 2 dpi). At these times, the majority (>90%; Fones *et al.*, 2017; Fantozzi *et al.*, 2021)  
 332 of virulent *Z. tritici* cells are still epiphytic, as are the cells of NIRP isolates, so that the interaction of  
 333 all isolates with the host is similar, and might be expected to provoke similar defence responses. At  
 334 14 dpi, however, the NBT response was higher towards the fully virulent isolates, supporting the  
 335 observation that only these isolates had penetrated the leaves. The greater superoxide response to  
 336 NIRP isolates at 1 dpi might indicate early detection of these isolates. We speculate that this  
 337 response to NIRP isolates may play a role in inducing the defences that both cause the necrosis  
 338 induction seen in response to NIRP isolates and prevent them from successfully invading the leaves.  
 339 This possibility should be investigated further. qPCR of *Z. tritici* specific DNA in washed (Fones *et al.*,  
 340 2017) and unwashed leaf samples supported the finding from microscopy that NIRP isolates were  
 341 not, or were barely, detectable inside the leaf at either 7 or 14 dpi (Fig 5). However, in unwashed  
 342 leaf samples, up to 4x as much *Z. tritici* DNA was found for NIRP than for fully virulent isolates (Fig.  
 343 5B). This counter-intuitive result indicates that NIRP isolates are not only surviving on the leaf  
 344 surface but proliferating. Further, this increase in fungal biomass on the leaf surface is not slow and  
 345 limited, but in fact outstrips the increase in biomass of virulent isolates at 14 dpi. At this time, the  
 346 fully virulent isolates have entered the apoplast and are beginning to colonise the mesophyll tissues,  
 347 but the switch to necrotrophic growth is yet to occur (Keon *et al.*, 2007; Yang *et al.*, 2013; Rudd *et al.*,  
 348 2015). Thus, these isolates are acting as biotrophs. This early biotrophic leaf invasion is known to  
 349 be associated with minimal increases in detectable biomass (Kema *et al.*, 1966; Rudd *et al.*, 2015)  
 350 and production of effectors and toxins to suppress plant immunity and facilitate the development of  
 351 infection (Zhong *et al.*, 2017; Kettles *et al.*, 2018; Meile *et al.*, 2018). Epiphytic growth in the NIRP  
 352 isolates therefore appears to be following a different developmental programme. With less exposure  
 353 to plant defences and less requirement for 'stealth' (Goodwin *et al.*, 2011), growth and reproduction  
 354 may be released from the constraints associated with early biotrophic infection, and instead mainly  
 355 constrained by other factors such as nutrient availability. While this apparent advantage is short-  
 356 lived, as isolates that remain on the leaf surface cannot access apoplastic nutrients and do not  
 357 produce pycnidiospores, it is possible that epiphytic proliferation in isolates that cannot colonise the  
 358 apoplast may underpin the reported ability of avirulent isolates to cross with both virulent and other  
 359 avirulent isolates *in planta* (Kema *et al.*, 2018; Orellana-Torrejon *et al.*, 2022). If 'avirulent' isolates  
 360 show the NIRP phenotype, then epiphytic proliferation may well provide a mechanism by which  
 361 'avirulent' isolates can be maintained in a field population of *Z. tritici*, even in the face of

362 monoculture of elite, resistant wheat cultivars. This suggestion is in line with the findings of  
363 Orellana-Torrejon *et al.* (2022). These authors found that 3.3% of *Z. tritici* isolates sampled from STB  
364 lesions in the field carried the avirulence gene *Stb16q*, recognised by the host cultivar. They  
365 suggested that maintenance of the avirulent isolates as epiphytes may have allowed their survival  
366 until the point where infection by virulent isolates caused the systemic induced susceptibility  
367 described by Seybold *et al.* (2020), allowing the avirulent isolate to infect (Orellana-Torrejon *et al.*,  
368 2022). It would be of great interest to determine whether the *Stb16q* carrier isolates show the NIRP  
369 phenotype on resistant wheat. These findings together highlight the potential implications of  
370 epiphytic survival and the NIRP phenotype for the population genetics of *Z. tritici*, especially  
371 considering its highly plastic genome and the existence of dispensible chromosomes in this species  
372 (Pope *et al.*, 2015; Plissonneau *et al.*, 2018; Graundaubert *et al.*, 2019; Lorrain *et al.*, 2021). In  
373 particular, the maintenance of NIRP isolates may maintain genetic diversity, potentially including a  
374 range of virulence determinants and fungicide or other stress resistance determinants that could be  
375 particularly significant for crop protection and fungal evolution under selection pressures such as  
376 changing wheat cultivars, changing climate, and fungicide usage.

### 377 **NIRP isolates rapidly trigger wheat defence signalling while on the leaf surface.**

378 Nitroblue tetrazolium (NBT) staining experiments (Fig 6) indicate that the wheat plant responds to  
379 the presence *Z. tritici* on the leaf surface rapidly by the production of superoxide. At 1 dpi, this  
380 response is higher for NIRP than for fully virulent isolates, with this discrepancy reducing in size so  
381 that it is not significant at 2 or 7 dpi, and then reversing. By 14 dpi, the response to fully virulent  
382 isolates is significantly higher than for NIRP isolates, though the overall response is much lower than  
383 that seen initially (Fig 6). It is likely that the response to fully virulent isolates reflects penetration  
384 and the early stages of apoplast colonisation, which are known to induce defence responses (Keon *et al.*  
385 *et al.*, 2007). Corroborating this, we see an upregulation of the  $\beta$ -1,3-glucanase gene in response to  
386 fully virulent isolates, but not to NIRP isolates at 14 dpi (Fig S1). This defence gene has previously  
387 been reported to show induction following apoplastic colonisation by *Z. tritici* (Shetty *et al.*, 2003;  
388 Keon *et al.*, 2007; Rudd *et al.*, 2015). The NIRP isolates do not colonise the apoplast and do not  
389 induce the expression of this defence gene. Similarly, NIRP isolates only induce an oxidative burst for  
390 the first 2 dpi. Although little is known about the interaction between wheat defences and surface-  
391 colonising *Z. tritici*, it has previously been reported that defences are upregulated within hours of  
392 inoculation (Rudd *et al.*, 2015), as well as throughout the early infection period and that these  
393 responses differ between virulent and avirulent isolates (Shetty *et al.*, 2009; Rudd *et al.*, 2015; Ma *et al.*  
394 *et al.*, 2018). This indicates that all *Z. tritici* isolates are recognised, but that the virulent and avirulent  
395 fungus induces differing responses. Early defence responses against NIRP isolates may explain why  
396 these isolates cause necrosis in Galaxie despite being unable to invade the leaves. Possible reasons  
397 for the different defence responses include i) differences in effector production; ii) differences in  
398 toxin production; iii) differences in avirulence gene complement and iv) differences in early  
399 penetration attempt rates. There are a relatively small number of well-characterised effector  
400 proteins in *Z. tritici*, and most of those that whose functions are understood have their highest  
401 expression at around 10-14 dpi, during the transition from biotrophic to necrotrophic growth  
402 (Marshall *et al.*, 2011; Meile *et al.*, 2018; Tian *et al.*, 2021). However, effectors that have a role in  
403 masking the presence of the fungus are expressed somewhat earlier. In particular, *in planta*  
404 expression of chitin binding LysM proteins peaks at 4-10 dpi, with expression therefore largely  
405 limited to the symptomless phase (Marshall *et al.*, 2011; Tian *et al.*, 2021). Isolate IPO323, used in  
406 both these studies, is predominantly undergoing exploratory surface growth at these times (Fones *et al.*  
407 *et al.*, 2017; Fantozzi *et al.*, 2021). Thus, LysM is expressed by epiphytic fungus, indicating that *Z. tritici*  
408 requires protection from either recognition or defensive chitinase while epiphytic. A number of  
409 PAMPs from fungi are known to be recognised by plants, including mannans, glucans and  
410 ergosterols, as well as chitin (Kettles & Kanyuka, 2016). One possibility, suggested by the significantly  
411 higher superoxide response seen here to NIRP than FV isolates at 1 dpi is therefore that NIRP

412 isolates are detected within the first hours or days of colonisation and that this detection induces or  
413 primes defence gene expression such that invasive growth becomes impossible, although epiphytic  
414 growth is not suppressed. A ribonuclease toxin, *Zt6*, which can cleave plant, animal, fungal and  
415 bacterial RNA, is secreted by *Z. tritici* from germination for around 4 days, as well as a second phase  
416 of production during the switch to necrotrophy (Kettles *et al.*, 2018). It is possible that this or  
417 another secreted toxin is detected by the host or has an effect upon the plant defence response to *Z.*  
418 *tritici*. Similarly, avirulence genes may be involved in plant detection of and early response to *Z.*  
419 *tritici*. *Z. tritici* avirulence proteins such as *AvrStb6* (Zhong *et al.*, 2017) and *Avr3D1* (Meile *et al.*,  
420 2018), have been shown to be repressed during growth *in vitro*, and derepressed *in planta*, as a  
421 result of chromatin remodelling following an unknown host signal (Meile *et al.*, 2020). In some cells,  
422 de-repression of effector gene expression occurred during epiphytic growth (Meile *et al.*, 2020). This  
423 demonstrates that *Z. tritici* undergoes some form of transcriptional reprogramming in response to  
424 host signals, and it is possible that host responses to different effector or toxin complements could  
425 be sufficiently different for NIRP isolates as to induce a transcriptional programme geared towards  
426 epiphytic growth and reproduction in the absence of the opportunity to infect. That host responses  
427 to epiphytic growth of NIRP isolates occur is clear from the necrosis seen in the host. Which, or  
428 which combination, of the pathways discussed here are involved remains an open question. It will  
429 also be interesting to determine how this host response to NIRP isolates interacts with the systemic  
430 acquired susceptibility caused by virulent isolates (Seybold *et al.*, 2020) in the case of co-infection.

431 Together, the results presented here show that *Z. tritici* is able to thrive as an epiphyte in the  
432 absence of a compatible host. This has implications for the maintenance of genetic variation within  
433 the pathogen population. It may thus be a factor in the evolution of virulence, fungicide resistance,  
434 tolerance of stresses such as those imposed by climate change, and other agronomically relevant  
435 traits.

436 **Acknowledgements:** The authors thank Dr Sreedhar Kilaru for the kind provision of GFP-tagged  
437 isolates and the University of Exeter Sequencing Service for producing sequence data.

438 **Author Contributions:** HF designed research, performed experiments, analysed data and wrote  
439 them paper. DS carried out genome alignments and SNP calling. SG designed research.

#### 440 **References**

441 Abràmoff, M. D., Magalhães, P. J., & Ram, S. J. (2004). Image processing with ImageJ. *Biophotonics*  
442 *International*, 11(7), 36-42.

443 Battache, M., Lebrun, M. H., Sakai, K., Soudière, O., Cambon, F., Langin, T., & Saintenac, C. (2022).  
444 Blocked at the Stomatal Gate, a Key Step of Wheat Stb16q-Mediated Resistance to Zymoseptoria  
445 tritici. *Frontiers in Plant Science*, 13.

446 Brown, J. K., Chartrain, L., Lasserre-Zuber, P., & Saintenac, C. (2015). Genetics of resistance to  
447 Zymoseptoria tritici and applications to wheat breeding. *Fungal Genetics and Biology*, 79, 33-41.

448 Fantozzi, E., Kilaru, S., Gurr, S. J., & Steinberg, G. (2021). Asynchronous development of  
449 Zymoseptoria tritici infection in wheat. *Fungal Genetics and Biology*, 146, 103504.

450 Feurtey, A., Lorrain, C., Croll, D., Eschenbrenner, C., Freitag, M., Habig, M., Haueisen, J., Möller, M.,  
451 Schotanus, K. & Stukenbrock, E. H. (2020). Genome compartmentalization predates species  
452 divergence in the plant pathogen genus *Zymoseptoria*. *BMC genomics*, 21(1), 1-15.

453 Fones, H., & Gurr, S. (2015). The impact of Septoria tritici Blotch disease on wheat: An EU  
454 perspective. *Fungal Genetics and Biology*, 79, 3-7.

- 455 Fones, H. N., Eyles, C. J., Kay, W., Cowper, J., & Gurr, S. J. (2017). A role for random, humidity-  
456 dependent epiphytic growth prior to invasion of wheat by *Zymoseptoria tritici*. *Fungal Genetics and*  
457 *Biology*, 106, 51-60.
- 458 Francisco, C. S., Ma, X., Zwyszig, M. M., McDonald, B. A., & Palma-Guerrero, J. (2019). Morphological  
459 changes in response to environmental stresses in the fungal plant pathogen *Zymoseptoria*  
460 *tritici*. *Scientific Reports*, 9(1), 1-18.
- 461 Goodwin SB, van der Lee TA, Cavaletto JR, Te Lintel Hekkert B, Crane CF, Kema GH (2007).  
462 Identification and genetic mapping of highly polymorphic microsatellite loci from an EST database of  
463 the septoria tritici blotch pathogen *Mycosphaerella graminicola*. *Fungal Genetics and Biology*. 44,  
464 398-414.
- 465 Goodwin *et al.* (2011). Finished genome of the fungal wheat pathogen *Mycosphaerella graminicola*  
466 reveals dispensome structure, chromosome plasticity, and stealth pathogenesis. *PLoS Genetics*,  
467 e1002070.
- 468 Grandaubert, J., Dutheil, J. Y., & Stukenbrock, E. H. (2019). The genomic determinants of adaptive  
469 evolution in a fungal pathogen. *Evolution Letters*, 3(3), 299-312.
- 470 Guindon S., Dufayard J.F., Lefort V., Anisimova M., Hordijk W., Gascuel O. (2010). New Algorithms  
471 and Methods to Estimate Maximum-Likelihood Phylogenies: Assessing the Performance of PhyML  
472 3.0. *Systematic Biology* 59, 307-21.
- 473 Guo, J. R., Schnieder, F., & Verreet, J. A. (2006). Presymptomatic and quantitative detection of  
474 *Mycosphaerella graminicola* development in wheat using a real-time PCR assay. *FEMS Microbiology*  
475 *Letters*, 262(2), 223-229.
- 476 Habig, M., Quade, J., & Stukenbrock, E. H. (2017). Forward genetics approach reveals host genotype-  
477 dependent importance of accessory chromosomes in the fungal wheat pathogen *Zymoseptoria*  
478 *tritici*. *MBio*, 8(6), e01919-17.
- 479 Haueisen, J., Möller, M., Eschenbrenner, C. J., Grandaubert, J., Seybold, H., Adamiak, H., &  
480 Stukenbrock, E. H. (2019). Highly flexible infection programs in a specialized wheat  
481 pathogen. *Ecology and evolution*, 9(1), 275-294.
- 482 Head, S. R., Komori, H. K., LaMere, S. A., Whisenant, T., Van Nieuwerburgh, F., Salomon, D. R., &  
483 Ordoukhanian, P. (2014). Library construction for next-generation sequencing: overviews and  
484 challenges. *Biotechniques*, 56(2), 61-77.
- 485 Jarošová, J., & Kundu, J. K. (2010). Validation of reference genes as internal control for studying viral  
486 infections in cereals by quantitative real-time RT-PCR. *BMC Plant Biology*, 10, 1–9.
- 487 Kema, G. H., Yu D., Rijkenberg, F.H., Shaw, M. W. & Baayen, R. P. (1996). Histology of the  
488 pathogenesis of *Mycosphaerella graminicola* in wheat. *Phytopathology*, 86, 777–86.
- 489 Kema, G. H., Goodwin, S. B., Hamza, S., Verstappen, E. C., Cavaletto, J. R., Van der Lee, T. A., de  
490 Weerd, M., Bonants, P. J., Waalwijk, C. (2002). A combined amplified fragment length  
491 polymorphism and randomly amplified polymorphism DNA genetic kinkage map of *Mycosphaerella*  
492 *graminicola*, the septoria tritici leaf blotch pathogen of wheat. *Genetics*, 161, 1497-505.
- 493 Kema, G. H., Mirzadi Gohari, A., Aouini, L., Gibriel, H. A., Ware, S. B., van Den Bosch, F., Manning-  
494 Smith, R., Alonso-Chavez, V., Helps, J., Ben M'Barek, S., Mehrabi, R., Diaz-Trujillo, C., Zamani, E.,



- 495 Schouten, H. J., van der Lee, T. A. J., Waalwijk, C., de Waard, M. A., de Wit, P. J. G. M., Verstappen, E.  
496 C. P., Thomma, B. P. H. J., Meijer, H. J. G., & Seidl, M. F. (2018). Stress and sexual reproduction affect  
497 the dynamics of the wheat pathogen effector AvrStb6 and strobilurin resistance. *Nature*  
498 *genetics*, 50(3), 375-380.
- 499 Keon, J., Antoniw, J., Carzaniga, R., Deller, S., Ward, J. L., Baker, J. M., Beale, M.H., Hammond-Kosack,  
500 K. & Rudd, J. J. (2007). Transcriptional adaptation of *Mycosphaerella graminicola* to programmed cell  
501 death (PCD) of its susceptible wheat host. *Molecular Plant-Microbe Interactions*, 20(2), 178-193.
- 502 Kettles, G. J., & Kanyuka, K. (2016). Dissecting the molecular interactions between wheat and the  
503 fungal pathogen *Zymoseptoria tritici*. *Frontiers in Plant Science*, 7, 508.
- 504 Kettles, G. J., Bayon, C., Sparks, C. A., Canning, G., Kanyuka, K., & Rudd, J. J. (2018). Characterization  
505 of an antimicrobial and phytotoxic ribonuclease secreted by the fungal wheat pathogen  
506 *Zymoseptoria tritici*. *New Phytologist*, 217(1), 320-331.
- 507 Kilaru, S., Schuster, M., Latz, M., Gupta, S. D., Steinberg, N., Fones, H., Gurr, S. J. & Steinberg, G.  
508 (2015). A gene locus for targeted ectopic gene integration in *Zymoseptoria tritici*. *Fungal Genetics*  
509 *and Biology*, 79, 118-124.
- 510 Larionov, A., Krause, A., & Miller, W. (2005). A standard curve based method for relative real time  
511 PCR data processing. *BMC Bioinformatics*, 6(1), 1-16.
- 512 Li, H., and Durbin, R. (2009). Fast and accurate short read alignment with Burrows-Wheeler  
513 transform. *Bioinformatics* 25,1754-1760.
- 514 Li, H. (2011). A statistical framework for SNP calling, mutation discovery, association mapping and  
515 population genetical parameter estimation from sequencing data. *Bioinformatics* 27, 2987-2993.
- 516 Linde, C. C., Zhan, J., & McDonald, B. A. (2002). Population structure of *Mycosphaerella graminicola*:  
517 from lesions to continents. *Phytopathology*, 92(9), 946-955.
- 518 Lorrain, C., Feurtey, A., Möller, M., Haueisen, J. and Stukenbrock, E., 2021. Dynamics of transposable  
519 elements in recently diverged fungal pathogens: lineage-specific transposable element content and  
520 efficiency of genome defenses. *G3*, 11(4), p.jkab068.
- 521 Love, A.J., Yun, B.W., Laval, V., Loake, G.J. & Milner, J. J. (2005). Cauliflower mosaic virus, a  
522 compatible pathogen of *Arabidopsis*, engages three distinct defense signaling pathways and  
523 activates rapid systemic generation of reactive oxygen species. *Plant Physiology* 139, 935-948.
- 524 Ma, X., Keller, B., McDonald, B. A., Palma-Guerrero, J., & Wicker, T. (2018). Comparative  
525 transcriptomics reveals how wheat responds to infection by *Zymoseptoria tritici*. *Molecular Plant-*  
526 *Microbe Interactions*, 31(4), 420-431.
- 527 Marshall, R., Kombrink, A., Motteram, J., Loza-Reyes, E., Lucas, J., Hammond-Kosack, K. E., Thomma,  
528 P. J. H. & Rudd, J. J. (2011). Analysis of two in planta expressed LysM effector homologs from the  
529 fungus *Mycosphaerella graminicola* reveals novel functional properties and varying contributions to  
530 virulence on wheat. *Plant Physiology*, 156(2), 756-769.
- 531 Meile, L., Croll, D., Brunner, P. C., Plissonneau, C., Hartmann, F. E., McDonald, B. A., &  
532 Sánchez-Vallet, A. (2018). A fungal avirulence factor encoded in a highly plastic genomic region  
533 triggers partial resistance to septoria tritici blotch. *New Phytologist*, 219(3), 1048-1061.



- 534 Meile, L., Peter, J., Puccetti, G., Alassimone, J., McDonald, B. A., & Sánchez-Vallet, A. (2020).  
535 Chromatin dynamics contribute to the spatiotemporal expression pattern of virulence genes in a  
536 fungal plant pathogen. *MBio*, *11*(5), e02343-20.
- 537 Mekonnen, T., Sneller, C. H., Haileselassie, T., Ziyomo, C., Abeyo, B. G., Goodwin, S. B., ... & Tesfaye,  
538 K. (2021). Genome-wide association study reveals novel genetic loci for quantitative resistance to  
539 septoria tritici blotch in wheat (*Triticum aestivum* L.). *Frontiers in plant science*, *12*, 671323.
- 540 O'Driscoll, A., Doohan, F., & Mullins, E. (2015). Exploring the utility of *Brachypodium distachyon* as a  
541 model pathosystem for the wheat pathogen *Zymoseptoria tritici*. *BMC Research Notes*, *8*(1), 1-10.
- 542 Orellana-Torrejon, C., Vidal, T., Gazeau, G., Boixel, A. L., Gélisse, S., Lageyre, J., Saint-Jean, S. &  
543 Suffert, F. (2022). Multiple scenarios for sexual crosses in the fungal pathogen *Zymoseptoria tritici* on  
544 wheat residues: potential consequences for virulence gene transmission. *Fungal Genetics and*  
545 *Biology*, *163*, 103744.
- 546 Plissonneau, C., Hartmann, F. E., & Croll, D. (2018). Pangenome analyses of the wheat pathogen  
547 *Zymoseptoria tritici* reveal the structural basis of a highly plastic eukaryotic genome. *BMC*  
548 *biology*, *16*(1), 1-16.
- 549 Poppe, S., Dorsheimer, L., Happel, P., & Stukenbrock, E. H. (2015). Rapidly evolving genes are key  
550 players in host specialization and virulence of the fungal wheat pathogen *Zymoseptoria tritici*  
551 (*Mycosphaerella graminicola*). *PLoS pathogens*, *11*(7), e1005055.
- 552 Rudd, J. J., Kanyuka, K., Hassani-Pak, K., Derbyshire, M., Andongabo, A., Devonshire, J., Lysenko, A.,  
553 Saqi, M., Desai, N.M., Powers, S.J., Hooper, J., Ambroso, L., Barti, A., Framer, A., Hammond-Kossack,  
554 K.E., Dietrich, R. A., & Courbot, M. (2015). Transcriptome and metabolite profiling of the infection  
555 cycle of *Zymoseptoria tritici* on wheat reveals a biphasic interaction with plant immunity involving  
556 differential pathogen chromosomal contributions and a variation on the hemibiotrophic lifestyle  
557 definition. *Plant Physiology*, *167*(3), 1158-1185.
- 558 Saintenac, C., Lee, W. S., Cambon, F., Rudd, J. J., King, R. C., Marande, W., Powers, S.J., Bergès, H.,  
559 Phillips, A.L., Uauy, C., Hammond-Kosack, K.E., Langin, T. & Kanyuka, K. (2018). Wheat receptor-  
560 kinase-like protein Stb6 controls gene-for-gene resistance to fungal pathogen *Zymoseptoria*  
561 *tritici*. *Nature Genetics*, *50*(3), 368-374.
- 562
- 563 Seybold, H., Demetrowitsch, T. J., Hassani, M. A., Szymczak, S., Reim, E., Haueisen, J., Lübbers, L.,  
564 Rühlemann, M., Franke, A., Schwarz, K. & Stukenbrock, E. H. (2020). A fungal pathogen induces  
565 systemic susceptibility and systemic shifts in wheat metabolome and microbiome  
566 composition. *Nature Communications*, *11*, 1910.
- 567 Shetty, N. P., Kristensen, B., Newman, M.-A., Møller, K., Gregersen, P. L. & Jørgensen, H. L. (2003).  
568 Association of hydrogen peroxide with restriction of *Septoria tritici* in resistant wheat. *Physiological*  
569 *and Molecular Plant Pathology*, *62*, 333-46.
- 570 Shetty, N. P., Jensen, J. D., Knudsen, A., Finnie, C., Geshi, N., Blennow, A., Collinge, D.B. & Jørgensen,  
571 H. J. L. (2009). Effects of  $\beta$ -1, 3-glucan from *Septoria tritici* on structural defence responses in  
572 wheat. *Journal of Experimental Botany*, *60*(15), 4287-4300.

- 573 Siah, A., Deweer, C., Duyme, F., Sanssené, J., Durand, R., Halama, P., & Reignault, P. (2010).  
 574 Correlation of in planta endo-beta-1, 4-xylanase activity with the necrotrophic phase of the  
 575 hemibiotrophic fungus *Mycosphaerella graminicola*. *Plant Pathology*, 59(4), 661-670.
- 576 Tian, H., MacKenzie, C. I., Rodriguez-Moreno, L., van den Berg, G. C., Chen, H., Rudd, J. J., Mesters, J.  
 577 R. & Thomma, B. P. (2021). Three LysM effectors of *Zymoseptoria tritici* collectively disarm  
 578 chitin-triggered plant immunity. *Molecular plant pathology*, 22(6), 683-693.
- 579 Yang, F., Li, W., & Jørgensen, H. J. (2013). Transcriptional reprogramming of wheat and the  
 580 hemibiotrophic pathogen *Septoria tritici* during two phases of the compatible interaction. *PLoS*  
 581 *One*, 8(11), e81606.
- 582 Yang, F., Li, W., Derbyshire, M., Larsen, M. R., Rudd, J. J. & Palmisano, G. (2015). Unraveling  
 583 incompatibility between wheat and the fungal pathogen *Zymoseptoria tritici* through apoplastic  
 584 proteomics. *BMC Genomics*, 16, 362.
- 585 Zhong, Z., Marcel, T. C., Hartmann, F. E., Ma, X., Plissonneau, C., Zala, M., Ducasse, A., Confais, J.,  
 586 Compain, J., Lapalu, N. and Amselem, J., MacDonald, B. A., Croll, D. & Palma-Guerrero, J. (2017). A  
 587 small secreted protein in *Zymoseptoria tritici* is responsible for avirulence on wheat cultivars carrying  
 588 the *Stb6* resistance gene. *New Phytologist*, 214(2), 619-631.

589

590 **Figure Legends**

591 **Figure 1: Differential development of symptoms in European vs American *Zymoseptoria tritici***  
 592 **strains on the European wheat variety Galaxie.** Leaves were inoculated with each isolate at  $10^7$   
 593 cfu/ml in 0.1% (v/v) Tween-20. A-C: Symptoms were assessed at 7, 14 and 21 days post inoculation  
 594 by randomly sampling 3 inoculated leaves for each strain, plus 3 control leaves. Sampled leaves were  
 595 photographed and the percentage area healthy, chlorotic or necrotic determined through image  
 596 analysis based on leaf colour. Letters above bars indicate significant differences in mean percentage  
 597 necrosis between isolates (ANOVA,  $P < 0.0001$ , with Tukey's simultaneous comparisons). D. Pycnidia  
 598 were counted at 28 days post inoculation on 4-12 inoculated leaves for each strain and control.  
 599 Values are means of three independent replicate experiments. Letters above bars indicate significant  
 600 differences between individual isolates (ANOVA,  $P < 0.0001$ , with Tukey's simultaneous  
 601 comparisons).

602 **Figure 2: Cryo- scanning electron and confocal laser scanning microscopy (cryo-SEM and CLSM)**  
 603 **images of *Z. tritici* strains on Galaxie wheat.** Leaves were inoculated with either wildtype (cryo-  
 604 SEM, rows 1&3) or strains of each isolate expressing cytosolic GFP (CLSM, rows 2&4) at  $10^7$  cfu per  
 605 ml. Representative images shown. Visible fungal cells (green) are on the leaf surface in all images  
 606 shown (confirmed by depth-coding of images as in Fones *et al.*, 2017) and background red colour  
 607 comes from chlorophyll autofluorescence in the underlying mesophyll cells. Arrowheads: blue -  
 608 exemplar epiphytic hyphae; yellow – exemplar epiphytic blastospores; pink – exemplar internal  
 609 hyphae. Scale bars represent 50  $\mu$ M.

610 **Figure 3: Representative images of the colonisation of the Galaxie leaf by IPO323 and T39.** Leaves  
 611 were inoculated with strains of each isolate expressing cytosolic GFP at  $10^7$  cfu per ml and imaged  
 612 using CLSM. Representative images shown. Visible fungal cells (green) are on the leaf surface in all  
 613 images until day 7 (confirmed by depth-coding of images as in Fones *et al.*, 2017) and are mainly  
 614 internal from day 10 in IPO323 but remain on the surface in T39. Background red colour comes from  
 615 chlorophyll autofluorescence in the underlying mesophyll cells until leaves became necrotic (15 dpi

616 onwards, IPO323 only) when 0.05% (w/v) propidium iodide (PI) was added to counterstain dead leaf  
 617 cells. Arrowheads: blue - exemplar epiphytic hyphae; yellow – exemplar epiphytic blastospores; pink  
 618 – exemplar internal hyphae.

619 **Figure 4: Germination and leaf penetration by *Z. tritici* isolates.** Leaves of Galaxie wheat were  
 620 inoculated with the GFP-expressing strain of each isolate at  $10^7$  cfu/ml. Initial inoculum consisted of  
 621 filtered blastospores and so was composed of yeast-like cells. At 3, 7 and 10 dpi, cells were imaged  
 622 by confocal microscopy. Isolates virulent on Galaxie are shown in blues while isolates avirulent on  
 623 Galaxie are shown in reds/oranges. Percentages shown are mean results from an average of 160 (31-  
 624 527) individual fungi analysed from an average of 7 (3-10) images collected per data point. Imaged  
 625 locations on the leaf were selected at random, but randomly selected locations containing no fungi  
 626 were not imaged. A: Percentage of fungal individuals with at least one hyphal cell during early  
 627 colonisation by each isolate. Imaged fungi were scored as having hyphal growth if at least one cell  
 628 was hyphal, regardless of the total number of cells present in the individual structure. The  
 629 percentage of individuals with hyphal growth thus reflects germination of blastospores and/or a  
 630 switch from yeast-like to hyphal growth on the leaf. Differences in rate of hyphal emergence could  
 631 be detected between isolates as soon as 3 dpi (ANOVA,  $p = 0.04525$ ). However, no significant  
 632 differences were found in the mean rate of hyphal formation in FV vs NIRP isolates at any of the time  
 633 points analysed ( $t$ -tests comparing means of isolate groups: 3 dpi,  $p = 0.27$ ; 7 dpi,  $p = 0.96$ ; 10 dpi,  $p$   
 634  $= 0.63$ ). Data are only shown until 10 dpi, after which crowding of the leaf surface made  
 635 differentiation of individual fungi impossible. B: Percentage of fungal individuals which are entirely  
 636 on the leaf surface. Imaged fungi were scored as internal if at least one cell was internal, regardless  
 637 of the total number of cells present in the individual structure. Significant differences in the rate of  
 638 leaf penetration were found at 10 dpi and 12 dpi ( $t$ -tests comparing means of isolate groups: 10 dpi,  
 639  $p = 0.0339$ ; 12 dpi,  $p = 0.0495$ ). These results reflect the lack of penetration by the three  
 640 NIRP isolates. Data are only shown until day 12 because separation of internal IPO323 (the fastest  
 641 colonising isolate) into distinct individuals became impossible subsequently. Data are means and  
 642 error bars show SE. Asterisks represent significant differences between isolate groups.

643 **Figure 5: quantitative PCR for detection of virulent vs avirulent *Z. tritici* isolates *in planta* on**  
 644 **Galaxie wheat.** Leaves of Galaxie were inoculated with each isolate at  $10^7$  cfu/ml and kept under  
 645 standard conditions until day 7 (A) or day 14 (B), before two leaves were sampled from each of  
 646 twelve plants. Half of the sampled leaves were washed in 0.1% (v/v) Tween-20. Following DNA  
 647 extraction, DNA was quantified and *Z. tritici* specific primers used to determine the proportion of  
 648 DNA in each sample that belonged to the fungus. At 7 dpi, there is little *Z. tritici* DNA in any sample  
 649 and washing reduces DNA detection for all isolates (A; ANOVA,  $p < 0.0001$ ), indicating *Z. tritici*  
 650 remained on the leaf surface. By 14 dpi, only NIRP isolates could be washed from the leaf surface to  
 651 give a significant drop in *Z. tritici* DNA detection (B: ANOVAs – NIRP,  $p < 0.0001$ ; FV,  $p = 0.995$ ).  
 652 However, NIRP isolates showed more *Z. tritici* DNA in unwashed samples, indicating surface  
 653 proliferation had occurred (B: ANOVA  $p < 0.0001$ ). Values are means and error bars show SE.  
 654 Asterisks indicate significant differences between the indicated isolate groups (\*  $p < 0.05$ ; \*\*  $p <$   
 655  $0.01$ , \*\*\*  $p < 0.001$ ).

656 **Figure 6: ROS signalling in wheat leaves in response to FV and NIRP isolates.** Leaves of Galaxie  
 657 wheat were inoculated with the GFP-expressing strain of each isolate at  $10^7$  cfu/ml. At 3, 7 and 10  
 658 dpi, leaves were harvested and stained with 0.1% (w/v) nitroblue tetrazolium (NBT), scanned, and  
 659 the percentage leaf area stained blue calculated by image analysis. Data are mean values for % NBT  
 660 staining across all FV or NIRP isolates in three independent repeat experiments. Error bars show SE.  
 661 Asterisks represent significance levels in ANOVAs comparing means of the three experiments for FV  
 662 vs NIRP isolate pools at each time point (1 dpi,  $p = 0.00282$ ; 2 dpi,  $p = 0.2257$ ; 7 dpi,  $p = 0.183$ ; 14  
 663 dpi,  $p = 0.00085$ ).

664 **Figure S1: Pseudosequence tree of isolates used in this study.** Bases at SNP sites were used to  
665 produce a pseudosequence for each strain, that was used to infer phylogenetic relationship  
666 Numbers at nodes represent bootstrap results. Only SNPs with a minimum read depth of 10 and 95%  
667 identity were included.

668 **Figure S2: Wheat defence responses against fully virulent and NIRP isolates.** Leaves of Galaxie  
669 wheat were inoculated with the GFP-expressing strain of each isolate at  $10^7$  cfu/ml. At 14 dpi, leaves  
670 were harvested used for RNA extraction and qRT-PCR of the defence gene  $\beta$ -1,3-glucanase. Data  
671 show mean values for fold change in gene expression vs uninoculated controls across all FV or NIRP  
672 isolates in or two independent repeat experiments. Error bars show SE.

673 **Table S1:** Primers used in this study.

674

675

#### 676 **Author Statement**

677 Helen N Fones: Investigation; Conceptualisation; Methodology; Visualisation; Writing – Original  
678 Draft; Writing - Review and Editing.

679 Darren Soanes: Formal Analysis

680 Sarah J Gurr: Resources; Writing - Review and Editing; Funding Acquisition

681

682 'Declarations of interest: none'.

683

#### 684 **Highlights**

- 685 • *Zymoseptoria tritici* isolates inoculated onto wheat on which they are not fully virulent are  
686 generally unable to enter the leaves, but instead proliferate epiphytically.
- 687 • These isolates induce early defence responses, leading to leaf necrosis, albeit to a lesser  
688 extent than seen in fully virulent isolates. They produce pycnidia very rarely, but not never.  
689 We named this isolate-cultivar interaction 'Necrosis-inducing with rare pycnidiation' (NIRP).
- 690 • Epiphytic growth by NIRP isoaltes can produce more biomass than early invasive growth  
691 during 'stealth biotrophy'.
- 692 • This advantage is later lost, because the NIRP isolates produce so few pycnidia in comparison  
693 to fully virulent isolates.
- 694 • We speculate that epiphytic proliferation in NIRP interactions may help to maintain the NIRP  
695 isolates' genes in field populations of *Z. tritici*.

696

697

698